Astron. Astrophys. 350, 617–625 (1999)

ASTRONOMY
AND
ASTROPHYSICS

Solar-like oscillations of Procyon A: stellar models and time series simulations versus observations⋆

C. Barban[1], E. Michel[1], M. Martic[2], J. Schmitt[2], J.C. Lebrun[2], A. Baglin[3], and J.L. Bertaux[2]

[1] Observatoire de Paris, DASGAL, CNRS UMR 8633, 92195 Meudon, France
[2] Service d'Aéronomie, CNRS, 91371 Verrières le Buisson, France
[3] Observatoire de Paris, DESPA, CNRS UMR 8632, 92195 Meudon, France

Received 9 July 1999 / Accepted 30 August 1999

Abstract. The aim of this paper is to discuss the possible stellar origin of the observed excess power presented in Martic et al. (1999) by comparing these observational data with theoretical predictions and numerical simulations. Stellar models are calculated for Procyon A with appropriate physics for this star and with the revised astrometric mass (1.46 ± 0.04) $M_\odot$ found by Girard (1998). For these models, we compute the expected oscillation spectra for ℓ=0,1,2 modes including m$\neq$0 according to theoretical amplitude predictions. Time-series are then simulated, in the same conditions as the observations, and compared by Fourier analysis with the observed ones. We show that the characteristics of the signal are in good agreement with what should be expected for such observing runs and we emphasize the importance of obtaining multi-site observations for this star. We confirm the presence of a periodic pattern in the Fourier spectrum, this pattern being interpreted as the so-called large separation.

Key words: stars: oscillations – stars: individual: Procyon A

1. Introduction

The great progress in understanding the internal structure of the Sun provided by helioseismology (the study of the interior of the Sun using its pulsations) has encouraged similar attempts to probe the internal structure of other stars. The detection of solar-like global acoustic oscillations (p-modes) in stars with different masses and ages will provide critical tests of the theory of stellar structure and evolution. Up to now, there has been no confirmed detection in any star but the Sun.

On the Sun, the maximum velocity amplitude in a single mode is about 20 cm s^{-1}. According to present theoretical estimates (e.g. Houdek et al. 1995), solar-like oscillations should be present in F to K stars on the main sequence with maximum amplitude around 2 m s^{-1} for early F stars. These amplitudes are small, at the edge of the photon noise of the available instrumentations. Therefore, the favourite targets are bright stars in order to get the adequate photon noise level and early-F stars for their larger expected oscillation amplitudes. Procyon A (α CMi, HD 61421, HR 2943), a F5 IV-V star, is one of the best target.

Oscillations with velocity amplitude around 1–2 m s^{-1} at the frequencies around 1 mHz are expected for this star (Houdek 1998, Kjeldsen & Bedding 1995). Furthermore, its brightness (m_V=0.34), its proximity (d=3.53 pc), and its binarity allow precise determinations of its fundamental stellar parameters (see Sect. 2).

From the ground, several attempts to detect solar-like oscillations on Procyon A have been made for more than a decade. The results obtained by Gelly et al. (1986) and Bedford et al. (1993) were not confirmed by later observations with greater sensitivity obtained by the same authors (see Innis et al. 1991, Bedford et al. 1995). Libbrecht (1988) and Innis et al. (1991) concluded that there was no evidence for solar-like oscillations at the precision of their data, i.e with a detection threshold for an isolated peak of ~ 1 m s^{-1} and ~ 4 m s^{-1}, respectively. Brown et al. (1991) observed an excess power between 0.3 and 1.4 mHz in the power spectrum of their data. They found maximum mode amplitudes of approximately 50 cm s^{-1} and some evidence for a large separation equal to 71 μHz. They emphasized, however, that the data do not permit a definitive estimate of the large separation since other values fit the observations about equally well. This result was discussed by Kjeldsen & Bedding (1995) who have been able to reproduce the Brown et al. (1991) observed power spectrum by merging white and non-white noise and using the same high-pass filter. Recently, Mosser et al. (1998) did not detect any significant excess in the power spectrum near 1 mHz. They reported a limit on the amplitude of the modes which does not exceed 1 m s^{-1}. However, they detected a possible regular pattern with a large separation equal to 53 μHz. The latest observations by Brown (1999) have shown an excess power of 0.4–0.5 (m s^{-1})^2 between approximately 0.5 and 1.5 mHz in the average of 4 power spectra computed from 4 different observing runs: February 1989, February 1997, February 1998 and March 1998.

Recent observations of Procyon A were made in November 98 using the fiber-fed echelle spectrograph ELODIE in an asteroseismological mode at the 193 cm telescope of the Observa-

Send offprint requests to: Caroline.Barban@obspm.fr

⋆ Based on observations collected at the Observatoire de Haute-Provence (CNRS, France).

toire de Haute-Provence (OHP). An excess power is observed in the Fourier space between 0.5 and 1.5 mHz (Martic et al. 1999), which confirms definitively the preliminary results obtained on a previous run in January 98 with the same equipment but with less quality data due to bad weather conditions and technical problems (Barban et al. 1999). This excess power, with a mean value of approximatively 0.4 $(\mathrm{m\,s^{-1}})^2$ over the best nights of data, is thought to be associated with solar-like oscillations.

The aim of this paper is to bring new evidences to the possible stellar origin of the observed signal presented in Martic et al. (1999). For this, we will compare the observational data with theoretical predictions and numerical simulations.

For the global parameters available for Procyon A and given in Sect. 2, we compute representative models for this star, with the code and the input physics described in Sect. 3. For these models, synthetic oscillation spectra are computed from p-modes frequency calculations and according to theoretical estimates of the expected amplitude. The main features of these oscillation spectra are presented and discussed in Sect. 4. Then, time series are simulated in the same conditions as the November 98 observations. In Sect. 5, these synthetic time series are compared with the observational ones via Fourier transform and a search for equidistances is made in the synthetic oscillation spectra and the observed one. Sect. 6 is devoted to conclusions.

2. Global parameters of Procyon A

We use the most up-to-date data related to the work of Girard et al. (1996) and Girard (1998) based on Yale PDS microdensitometer measurements of plates over 80 years and from two recent measurements of the separation of the two components A and B made by a new infrared coronograph (CoCo) and the WFPC2 Planetary Camera of the HST. This work gives a mass of (1.46 $\pm$ 0.04) $M_\odot$; this value is now in agreement with the mass estimated from stellar evolution (see Sect. 3 and Guenther & Demarque (1993)). A parallax Π=(0.2832 $\pm$ 0.0015) and an inclination of the orbit of the binary system to the line of sight, i=(58.9 $\pm$ 0.6)°, were also determined by Girard et al. (1996).

The effective temperature used in this paper, T_{eff}=(6530 $\pm$ 90) K, is a mean value, based on recent diameter measurements, established by Fuhrmann et al. (1997) with a direct method using bolometric magnitudes and average of integrated fluxes. This value is in agreement with the one found by recent spectroscopic measurements which give T_{eff}=(6480 $\pm$ 50) K where 50 K is the internal uncertainty (van't Veer-Menneret et al. 1998). Taking into account the uncertainty for the abundance of iron [Fe/H]=-0.07 $\pm$ 0.05 found by van't Veer-Menneret et al. (1998), we consider a solar abundance for this star.

We use the luminosity, log $L/L_\odot$=(0.86 $\pm$ 0.03), deduced from the parallax Π=(0.2832 $\pm$ 0.0015)" found by Girard et al. (1996) and the total integrated flux F=(18.64 $\pm$ 0.87) x 10^{-6} ergs $\mathrm{cm^{-2}\,s^{-1}}$ determined from optical, infrared and ultraviolet data (Smalley & Dworetsky 1995).

The projected rotational velocity considered in this paper is v sini=(4.9 $\pm$ 1) $\mathrm{km\,s^{-1}}$ (Fekel 1997). The value of the rotational velocity corresponding to the inclination found by Girard et al. (1996) is v=(5.72 $\pm$ 3.24) $\mathrm{km\,s^{-1}}$.

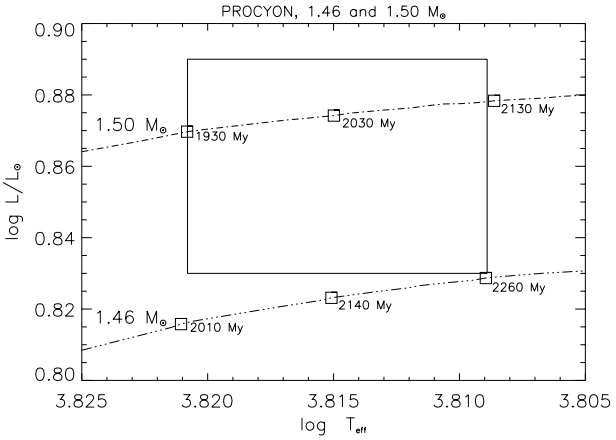

Fig. 1. HR diagram for Procyon A. The rectangle defines the 1 σ error box in effective temperature and luminosity. Evolutionary tracks are plotted with dash dot dot dot line for 1.46 $M_\odot$ and with dash dot line for 1.50 $M_\odot$.

3. Stellar models

Stellar models are calculated with the CESAM evolutionary code (Morel 1997). We use input physics appropriate to the considered mass. The nuclear reaction rates are from Caughlan & Fowler (1988). The equation of state is from Eggleton, Faulkner & Flannery (1973). The atmosphere is computed using Eddington's $T(\tau)$ law. We use the OPAL radiative opacities (Iglesias et al. 1992) complemented at low temperatures ($T \leq 10000$ K) by the Alexander & Ferguson data (1994). The mixture of heavy elements used in the opacity calculations is the solar mixture from Grevesse (1991). The isotopic ratios are the same as in Maeder (1983). Convection is described according to the classical mixing-length theory (Böhm - Vitense 1958) with a mixing-length, $l=\alpha H_p$ where H_p is the pressure scale-height. The mixing-length parameter has been chosen equal to the solar value, α=1.67, calibrated with the same physics. The unicity of α along the main sequence has been suggested by Fernandes et al. (1996), Perryman et al. (1998) and Lebreton et al. (1999). Models take into account an overshooting of the convective core over a distance of 0.20 H_p following the prescription of Schaller et al. (1992), confirmed by results obtained for the Hyades (Perryman et al. 1998).

We compute evolutionary tracks using this input physics and with a solar metallicity of Z = 0.019 within the range of mass introduced in Sect. 2, i.e. (1.46 $\pm$ 0.04) $M_\odot$. We notice that the two evolutionary tracks corresponding to 1.46 $M_\odot$ and 1.50 $M_\odot$ pass through or very near the error box in (T_{eff},L) in the HR diagram presented in Fig. 1. The set of models satisfying both constraints, i.e. the range of mass and the error box in (T_{eff},L), can reasonably be described by the masses 1.46 $M_\odot$ and 1.50 $M_\odot$ and by the ages 2010 to 2260 My and 1930 to 2130 My respectively. These models correspond to a late main sequence phase of core hydrogen burning (between 25 and 35%

Table 1. Rotational frequency ν_s, cut-off frequency ν_c, mean first-order spacing $\overline{\Delta\nu}$ for ℓ=0,1,2, mean second-order spacing $\overline{\delta\nu_0}$, spacing between ℓ=0 and ℓ=1 for a given n $\overline{\Delta\nu_1}$, for M=1.46 $M_\odot$ and for three models corresponding to a given age and a given radius.

Age (My)	log (R/$R_\odot$)	ν_s (μHz)	ν_c (mHz)	$\overline{\Delta\nu}$ (μHz)			$\overline{\delta\nu_0}$ (μHz)	$\overline{\Delta\nu_1}$ (μHz)
				ℓ=0	ℓ=1	ℓ=2		
2010	0.29	0.65	1.80	58.53	59.20	59.40	3.96	26.41
2140	0.30	0.63	1.66	55.92	56.52	56.41	3.59	24.87
2260	0.32	0.61	1.56	53.53	53.92	54.05	3.43	23.52

Table 2. Same as Table 1 for M=1.50 $M_\odot$.

Age (My)	log (R/$R_\odot$)	ν_s (μHz)	ν_c (mHz)	$\overline{\Delta\nu}$ (μHz)			$\overline{\delta\nu_0}$ (μHz)	$\overline{\Delta\nu_1}$ (μHz)
				ℓ=0	ℓ=1	ℓ=2		
1930	0.32	0.61	1.61	53.77	54.57	54.73	3.53	23.94
2030	0.33	0.59	1.52	51.80	52.28	52.48	3.34	22.81
2130	0.35	0.57	1.45	49.64	50.11	50.16	3.18	21.80

of hydrogen remains in the stellar core). The main difference between our models and those of Guenther & Demarque (1993) is the introduction of overshooting at the boundary of the convective core, which leads to a less evolved structure and a slightly higher mass at the same position in the HR diagram.

4. Theoretical oscillation spectra for Procyon A

For the stellar models described above, we calculate p-mode frequencies with the adiabatic oscillation code written by J. Christensen-Dalsgaard (here after JCD) (Christensen-Dalsgaard 1982), following recommendations by Christensen-Dalsgaard & Berthomieu (1991). The surface boundary condition is obtained by matching continuously the solution to the analytic solution of the adiabatic wave equation in an isothermal atmosphere (Unno et al. 1979).

Oscillation frequencies are calculated for ℓ=0,1,2 and m=0 in the frequency range defined by the fundamental radial mode and the cut-off frequency at the stellar surface, $f_c = \frac{1}{2\pi}\frac{c}{2H_p}$ where c is the adiabatic sound speed and H_p the pressure scale-height. The frequencies corresponding to m$\neq$0 are calculated using the simple first-order perturbative description of the rotational splitting, valid for slow rotation: $\mid \nu_{m,n,\ell} - \nu_{0,n,\ell} \mid = m\nu_s$. The rotational frequency ν_s = v / 2ΠR is determined from the rotational velocity given in Sect. 2 and the radius of our models (we assume that the rotational axis is perpendicular to the orbital plane of the binary system), see Tables 1 and 2.

The main features of these oscillation frequencies are: the cut-off frequency, the first order spacing (also called the large separation), $\Delta\nu(n,\ell) \simeq \nu(n+1,\ell) - \nu(n,\ell)$, the second order spacing (also called the small separation), $\delta\nu_0(n,\ell) = \nu(n+1,\ell=0) - \nu(n,\ell=2)$ and finally $\Delta\nu_1(n,\ell) \simeq \nu(n,\ell=1) - \nu(n,\ell=0)$.

The mean values of these quantities, determined from all the frequencies excluding the lower order frequencies for which the asymptotic approximation leading equidistances is not satisfied, are given in Tables 1 and 2 for three different representative ages for both evolutionary tracks presented for Procyon A.

The cut-off frequency ν_c, varies between 1.45 and 1.80 mHz. As showed by Audard et al. (1998), a refined treatment of the atmosphere might induce an increase of the cut-off frequency value up to about 8% of the standard cut-off frequency. This suggests for Procyon A a value of the cut-off frequency between 1.45 and 1.95 mHz.

The mean first order spacing $\overline{\Delta\nu}$ varies between approximately 49.5 and 60 μHz. This parameter brings global informations (essentially about the mean density) and as discussed also by Chaboyer et al. (1998) is not very discriminant in term of input physics. Let us note that very similar values are found in our models with overshooting and in those of Guenther & Demarque (1993) without overshooting i.e. with a different internal structure.

The mean second order spacing $\overline{\delta\nu_0}$ varies between approximately 3 and 4 μHz in our models. As shown by Guenther & Demarque (1993), the value of this parameter is ranging from 3 to 6 μHz for models of different input physics. The second order spacing is sensitive to the very innermost layers of the star, the knowledge of this parameter would be very interesting as commented in Guenther & Demarque (1993). Indeed this parameter might allow us to discriminate between different models corresponding to different evolutionary states and to different input physics.

The rotational frequency ν_s varies between 0.57 and 0.65 μHz. These values are low enough to legitimate the use of the first-order perturbative description of the rotational splitting as mentioned above. Even neglecting the intrinsic line width of the modes, we can notice that for observations spanning over less than 18 days, the different components of a given multiplet can not be resolved.

In order to construct theoretical oscillation spectra, we use the estimates of the expected amplitudes oscillations in main sequence stars of Houdek et al. (1999). From this work, Houdek (1998) predicts oscillation amplitudes for Procyon A around 1–2 m s^{-1} and a mode life times of a few days with a large uncertainty. The amplitude distribution has a bell shape similar to what is observed for the Sun with a maximum amplitude around

Table 3. Amplitude ratios between (ℓ=0,m=0) and the other modes.

ℓ,m	amplitude ratios
ℓ=0,m=0	1
ℓ=1,m=0	0.65
ℓ=1,m=-1,1	0.79
ℓ=2,m=0	0.11
ℓ=2,m=-1,1	0.47
ℓ=2,m=-2,2	0.41

1 mHz. We can explain schematically this amplitude shape for the lower frequencies by the decrease of the mode mass with increasing frequenc y and for the higher frequencies by the decreasing efficacity of the mode excitation by convection. For ℓ=0 modes, we mimic this amplitude distribution by a Gaussian shape, with a maximum amplitude of 1.5 m s^{-1} around 1 mHz and a FWHM of 0.84 mHz (see Fig. 2). We assume the same amplitude distribution for modes $\ell \neq 0$ since in the case of p modes the considered eigenfunctions are very similar for different ℓ (ℓ being small here) in the exte rnal layers where the excitation takes place. To mimic whole disk velocity observations, we apply to $\ell \neq 0$ modes visibility coefficients which take into account the inclination of the line of sight and the different geometrical contributions of the spherical harmonics (see appendix A). The resulting amplitude ratios between (ℓ=0,m=0) and the other modes are given in Table 3.

As an example, Figs. 2 and 3 represent the theoretical oscillation spectrum for the model corresponding to M=1.50 M$_\odot$ and 2030 My.

5. Confrontation between observed and predicted oscillations properties

5.1. Main characteristics of the observational data

The main characteristics of the excess power present in the power spectra calculated from the data obtained in November 98 (Martic et al. 1999) are the following:

a an excess power found between 0.5 and 1.5 mHz both in the power spectrum of the entire run calculated for the best nights and in the power spectra of individual nights (see for example Figs. 4a and 6); no peaks nor excess power exceeding the noise level are observed for $f \geq 1.5\ mHz$ (Fig. 4a).
b equidistant peaks at approximately (53 $\pm$ 3) μHz.
c irregular shape in power and a mean value of approximately 0.4 (m s^{-1})^2 with higher peaks up to approximately 0.9 (m s^{-1})^2 in the power spectrum of the entire run calculated for the best nights (Fig. 4b).
d very strong night to night changes of the mean power value and of the global shape (Fig. 6).

The calculated frequency range which appears in the theoretical oscillation power spectrum presented in Fig. 2 is in perfect agreement with the observed one. Indeed, this spectrum shows an important decrease of power around 0.5 and 1.5 mHz.

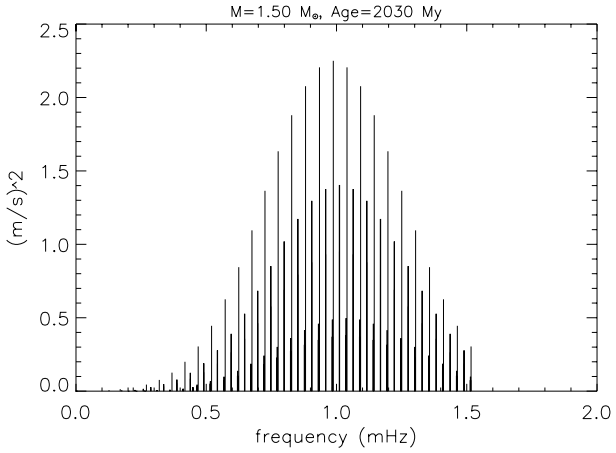

Fig. 2. Oscillation frequencies calculated with the JCD code for Procyon A. M=1.50 M$_\odot$, log T$_{eff}$ $\sim$ 3.8150, log L/L$_\odot$ $\sim$ 0.8742, Z=0.019, age=2030 My. The highest peaks correspond to ℓ=0, the intermediate ones to ℓ=1 and the smallest ones to ℓ=2.

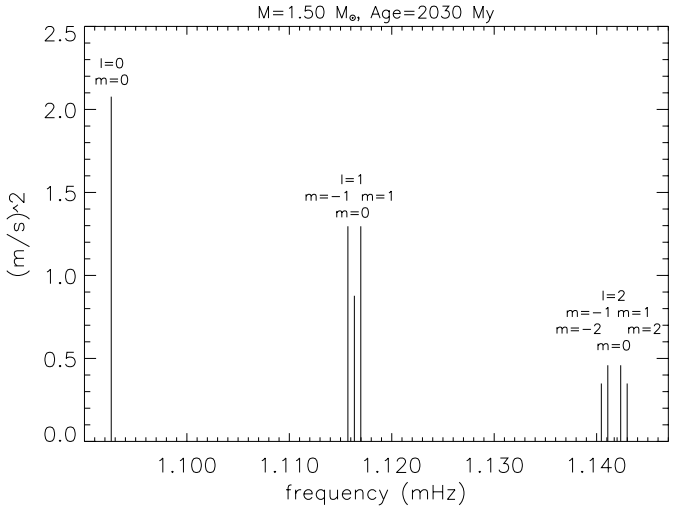

Fig. 3. A zoom of Fig. 2 for a given n.

The value of $\overline{\Delta\nu}$ found by Martic et al. (1999), i.e. (53 $\pm$ 3) μHz, is in the range of the theoretical values calculated for different set of models (see Tables 1 and 2).

We will show that the characteristics c and d can be reproduced by simulated time series taking into account the observational window.

5.2. Observational time series versus simulated ones, the role of the observational window

The mono-site observational window is characterized by a central peak which the FHWM is approximately the inverse of the total duration of the observations (this quantity is called resolution in the following) and by side-lobes due to the daily aliases, on both sides of the central peak at 11.57 μHz (1/24h) and at multiple of this value (see the window graph in Fig. 4). Close peaks will thus interfer through the central peak. Considering the daily aliases, we will see in this section that they play an important role through interferences between modes in the case

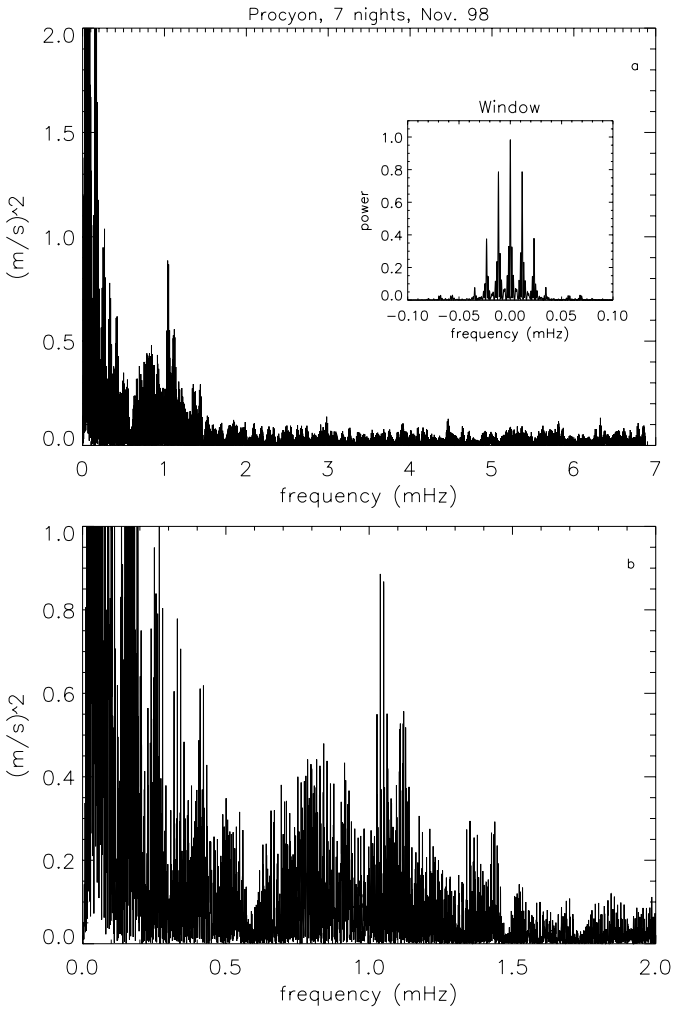

Fig. 4. a Power spectrum of Procyon A corresponding to the seven best nights merged together, i.e. 39.8311 h of data, (Nov. 7–8, Nov. 8–9, Nov. 9–10, Nov. 12–13, Nov. 14–15, Nov. 15–16, Nov. 16–17 1998). No filtering is made at low frequencies. The resolution is approximately 1.25 μHz as shown in the window spectra. (The Fourier transform is normalized by 2/N, where N is the number of the effective data). **b** A zoom of **a**.

of Procyon A and can explain the amplitude characteristics of the observed excess power.

5.2.1. Construction of simulated time series

Synthetic time series are simulated in the same conditions as the November 98 observations. These time series consist in a sum of sine-waves with frequencies and amplitudes corresponding to the synthetic oscillation spectrum of a given model. The sine-waves are given with arbitrary phases randomly distributed. These time series are multiplied by the observational window of the November 98 observations taking into account the exposure time and the sampling time of our observations. Before trying to explain the amplitude frequency variations in term of physical process, it is wise to look at the influence of the observational conditions. As commented by Kjeldsen et al. (1995) the instrumental noise can modify the observed amplitudes depending on the S/N ratio. Beyond this random effect, we will show here that the coincidence of the comb structure of both the Procyon A spectrum and the mono-site observational window produces systematic perturbations of the observed amplitude distribution. We concentrate here on the description of this effect which is important in the case of Procyon A. We thus consider that the amplitudes and the phases of the modes are constant over the observing period.

Considering the small variations of the values of the different parameters coming from our models (c.f Sect. 4), we will illustrate the observational effect on a representative model. The chosen model corresponds to 1.50 $M_\odot$ and 2030 My.

5.2.2. Amplitude characteristics

Some examples of power spectra of synthetic time series calculated with different randomly chosen sets of phases are presented in Fig. 5, showing that different sets of phases lead to significantly different shapes of the excess power.

The power spectra of the simulated time series are very different from the distribution of frequencies and amplitudes introduced in the simulation (see Fig. 2). This difference is only due to interferences between peaks through the observational window. Considering the FWHM of the central peak, i.e. 1.25 μHz, of the November 98 observations, we expect interferences between modes in a same multiplet only. But the mono-site strong aliases at 11.57 μHz and 23.04 μHz will play an important role in the case of Procyon A. Indeed, these values happen to be very close of respectively $0.5\overline{\Delta\nu_1}$ and $\overline{\Delta\nu_1}$ for all of our models within the data resolution. This coincidence generates strong interferences between ℓ=0 and ℓ=1, and ℓ=1 and ℓ=2 modes. All these interferences, in case of constructive interferences between peaks, are responsible for the maximum power, between 6 and 8 $(\mathrm{m\,s^{-1}})^2$, obtained in the power spectra of simulated time series (Fig. 5) while we injected a signal of 2.25 $(\mathrm{m\,s^{-1}})^2$.

The power spectra of the representative simulated time series (Fig. 5) reproduce well the irregular observed excess power (Fig. 4a), irregular shape due to the interferences mentioned above. The simulated power is greater than the observed one (Fig. 4a); this can be explained by an overestimate of the predicted amplitude but also by the work hypothesis that all the modes are excited at the same time over the observing period.

For a one-night observing run, the resolution is approximately 45 μHz leading to interferences between all the modes with the same n plus interferences with the nearest modes at n+1. A comparison between the observed one-night spectra and the simulated ones (Figs. 6 and 7) reveals amplitude changes of the same kind. We want to stress that in Fig. 7, the changes are only due to interferences between modes through the one-night resolution.

We remind that we do not introduce noise in our simulated spectra and that the noise can produce the same kind of effects that observational window interferences, with more or less importance depending on signal-to-noise ratio.

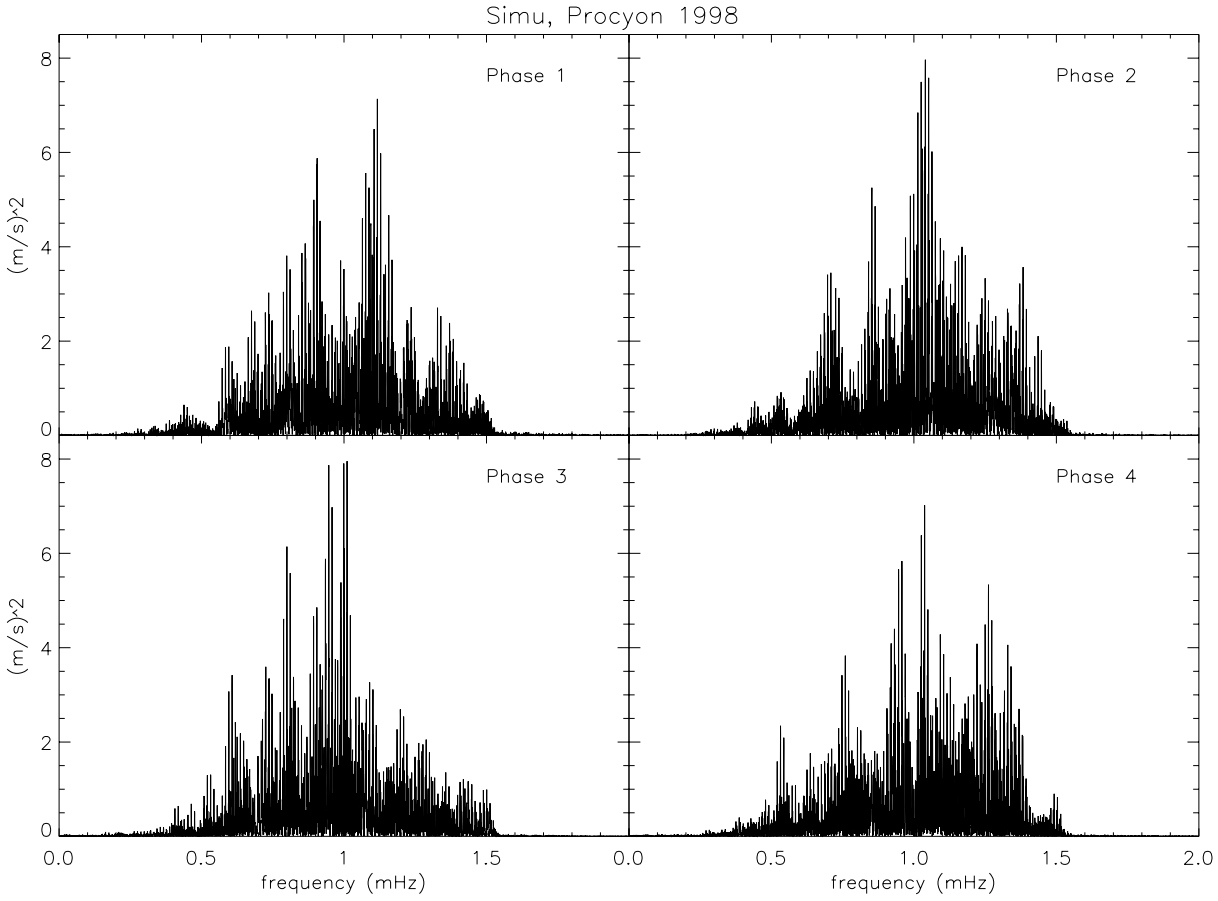

Fig. 5. Power spectra of simulated time series for a window corresponding to the 7 best nights obtained on Procyon A on Nov. 98 for 4 different sets of random phases; from a model of M=1.50 $M_\odot$ and age=2030 My (same normalization for the Fourier Transform that for Fig. 4).

5.2.3. Search for equidistant peaks

As discussed in Sect. 4, theoretical oscillation spectra show evenly distributed features responsible for several characteristic spacings ($\Delta\nu$, $\delta\nu_0$, $\Delta\nu_1$). To search for equidistances, we use the following method based on histogram, as already used in a slightly different way by Breger et al. (1999). We select the best signal-to-noise peaks of the spectrum. A new spectrum is build from the original one with the set of selected peaks and shifting the frequency origin to the frequency of the first selected peak. A second amplitude spectrum is build choosing for the frequency origin the frequency of the second selected peak; then this amplitude spectrum is added to the previous one. This process is repeated for all the selected peaks. A weighting factor is given each time, depending on the height of the peak.

In order to illustrate the method, we compute the histogram of the frequency spacings corresponding to a spectrum associated to continuous observations over a same time length that this of November 98 (i.e. approximately 222 h of data) for a model of 1.50 $M_\odot$ at 2030 My (Fig. 8). We can clearly see on this figure that equidistant peaks at $\sim$ 23, $\sim$ 26 and $\sim$ 50 μHz are present. These peaks are associated to $\overline{\Delta\nu_1}$, $\overline{\Delta\nu_1} + \overline{\delta\nu_0}$ and to $\overline{\Delta\nu}$ (see Table 2).

Then, to see the effect of the non-continuous observations, we calculate the histogram of the frequency spacings corresponding to the spectrum associated to the same model but simulated with the November 98 observational window (Fig. 9). The previous peaks seen in Fig. 8 corresponding to the considered model equidistances are present. The other peaks and especially the peak 1 at $\sim$ 11.5 μHz are due to the daily aliases.

It is interesting to see the results for another model for which we expect different values of quasi-equidistances. Then, we compute the histogram of the frequency spacings corresponding to the simulated amplitude spectrum associated to the 1.46 $M_\odot$ model at 2140 My (see Tables 1 for the expected equidistances). This histogram (Fig. 10) reveals that the peaks 1 and 2 are at the same frequencies for both figures. Peak 3 is severely perturbed by the peak 2. The other peaks have moved: in Fig. 9, peak 5 is present at $\sim$ 52 μHz with two other peaks (4 and 6) at $\pm \sim$ 11 μHz from the peak 5; for the Fig. 10, peak 5 is present at $\sim$ 56 μHz with two other peaks (4 and 6) at $\pm \sim$ 11 μHz from the peak 5.

We conclude that the values of $\overline{\Delta\nu}$ for the two models (i.e. $\sim$ 52 μHz and 56 μHz respectively) are nicely recovered despite the presence of the daily aliases. We notice that in these simulations, we can not distinguish $\overline{\Delta\nu_1}$ from the $\sim$ 23 μHz of the daily aliases and we can not detect the small separation. These

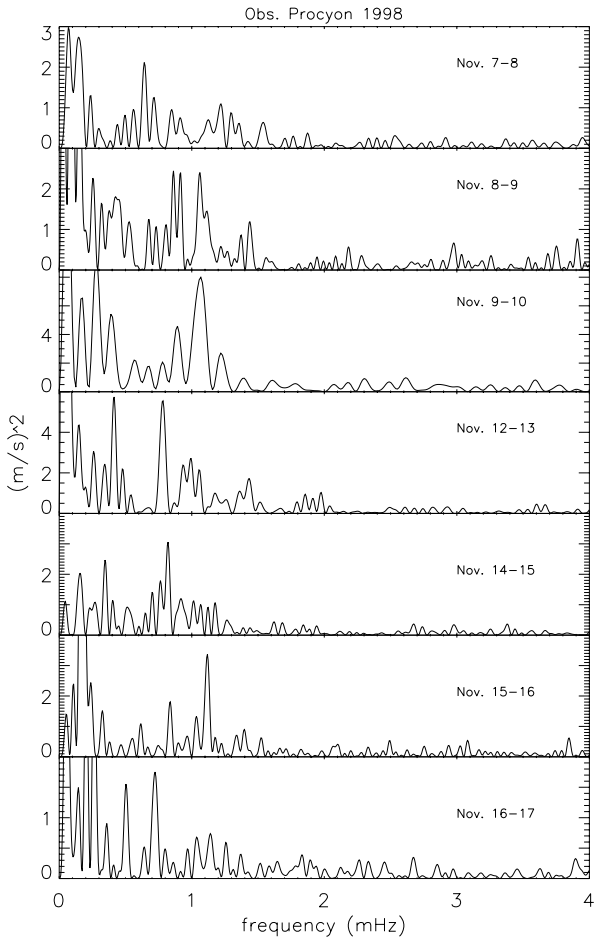

Fig. 6. Power spectrum of the radial velocity shifts of Procyon A obtained on Nov. 7–8 98 (Resolution (R)=50.32 μHz), on Nov. 8–9 98 (R=43.11 μHz), on Nov. 9–10 98 (R=100.56 μHz), on Nov. 12–13 98 (R=48.21 μHz), on Nov. 14–15 98 (R=41.85 μHz), on Nov. 15–16 98 (R=41.41 μHz), on Nov. 16–17 98 (R=46.31 μHz). No filtering is made at low frequencies.

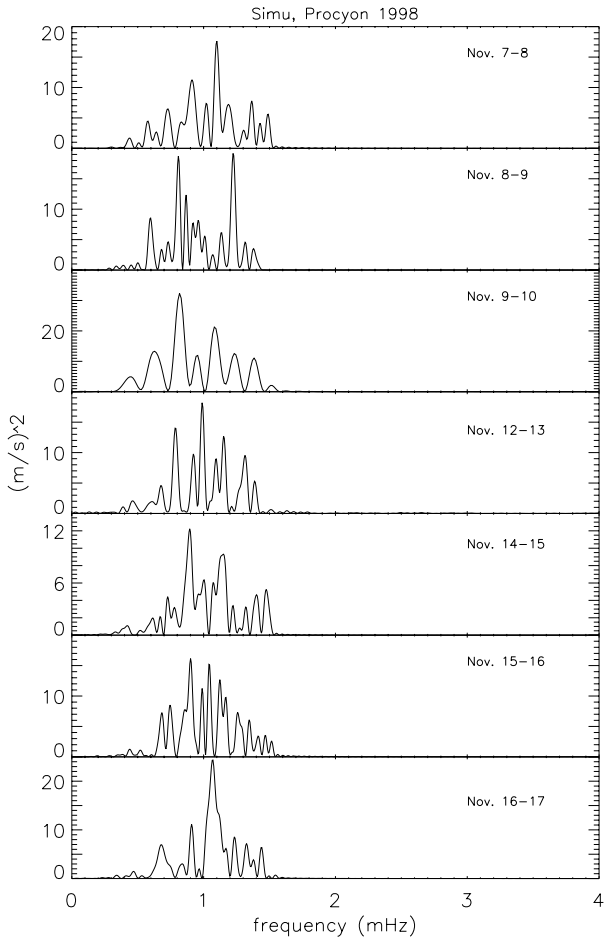

Fig. 7. Power spectra of simulated time series for a window corresponding to that of each of the 7 nights obtained on Procyon A on Nov. 98 from a model of M=1.50 $M_\odot$ and age=2030 My.

results show that the "histogram" method is able to extract $\overline{\Delta\nu}$ in Procyon A mono-site time series. We thus apply it to the real data.

Fig. 11 represents the histogram of the frequency spacings of the observational data. Peaks 1 and 2 at ~ 11.5 and 23 μHz do not move compared to Figs. 9 and 10. Peaks are present at ~ 56 μHz and $\sim 56 \pm 11.5$ μHz. The frequency of the peak 5, i.e. 56 μHz, is in perfect agreement with the $\overline{\Delta\nu}$ (see Tables 1 and 2) expected for this star. An identical value was obtained in the power spectra of two independent segments of 4 and 3 contiguous nights by Martic et al. (1999) using a Comb respons. The stellar origin of this quasi-equidistance is now firmly established.

6. Conclusion

In this paper, we bring new evidences to the stellar origin of the excess power observed on November 98 (Martic et al. 99). Stellar models are computed using an up to date physical representation of Procyon A. Then, synthetic oscillation spectra are obtained from p-mode frequencies calculation using these stellar models and available amplitude predictions. Simulated time series are computed from these synthetic spectra in the same conditions as the November 98 observations. The power spectrum of representative time series reproduces well the characteristics of the observed spectra. The observed frequency range of the excess power, i.e. 0.5–1.5 mHz, is in perfect agreement with the predicted one. The irregular shape of the excess power and night to night power variations, as already mentioned by Brown et al. 1991, can be explained by interferences between modes. We demonstrate that the value of approximately 56 μHz due to equidistant peaks in the power spectrum can be associated with the expected large separation of Procyon A.

We have thus demonstrated that an approximative value of a mean first order spacing can be determined from mono-site observations of Procyon A. This value is used here to comfort the stellar origin of the signal. Unfortunately, as commented in Sect. 4, the mean value of this parameter is not very sensitive to the input physics. On the contrary, the second order spacing, governed by the gradients of the sound speed in the inner core, would allow for instance to estimate the amount of overshooting. In addition to the low amplitudes of the considered modes, obtaining this parameter is difficult by the interferences between

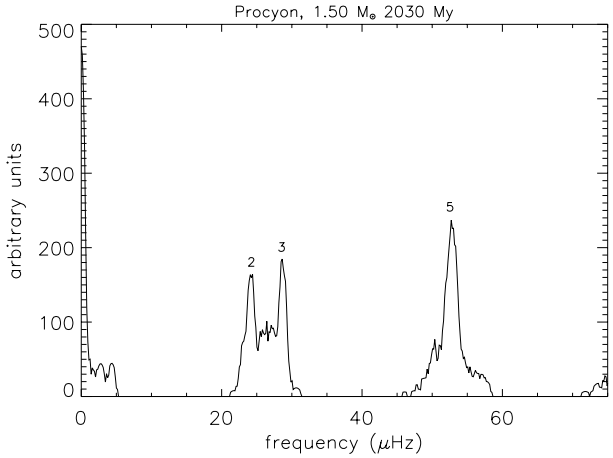

Fig. 8. Histogram of the frequency spacings corresponding to the amplitude spectrum calculated with a window corresponding to continuous observations over $\sim$ 222 h from the synthetic oscillation spectrum of the model for 1.50 $M_\odot$ at 2030 My.

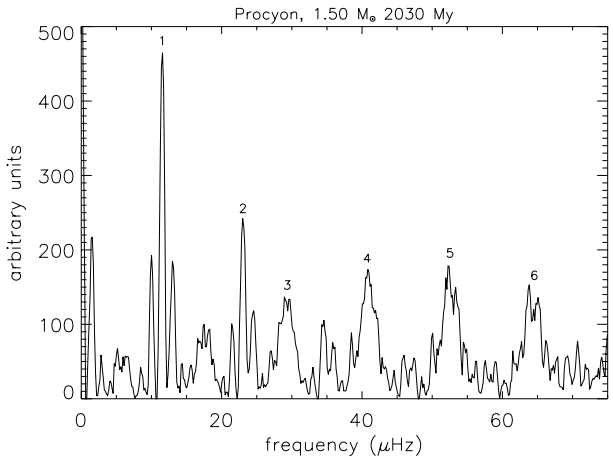

Fig. 9. Histogram of the frequency spacings corresponding to the amplitude spectrum calculated with the Nov. 98 window from the synthetic oscillation spectrum of the model for 1.50 $M_\odot$ at 2030 My.

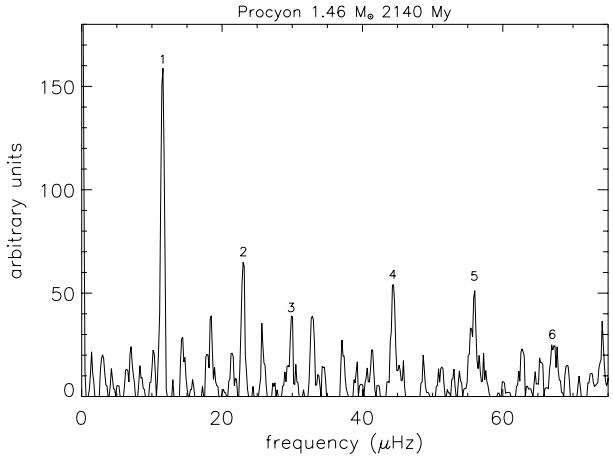

Fig. 10. Histogram of the frequency spacings corresponding to the amplitude spectrum calculated with the Nov. 98 window from the synthetic oscillation spectrum of the model for 1.46 $M_\odot$ at 2140 My.

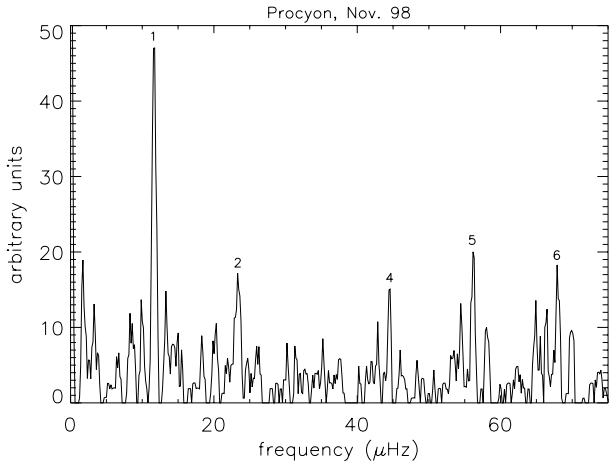

Fig. 11. Histogram of the frequency spacings corresponding to the amplitude spectrum obtained from the Nov. 98 data.

the ℓ=2 multiplet through the observational resolution and also by the interferences between ℓ=1 and ℓ=2 through the second daily alias.

Following this first result, the next significant step will be achieved through multi-site observations which reduce the amplitude of the daily aliases. Two instruments, the AFOE spectrograph (Brown 1999) and the ELODIE spectrograph in its asteroseismological mode, are capable of providing Doppler measurements with the required precision of a few m s^{-1} and have already given results of similar quality on Procyon A. Taking into account the improvement of the FTS mentioned in Mosser et al. (1998), it would also be interesting to combined the FTS data with the other two sites ones. A first multi-site campaign was organized in Feb. 99 using these three instruments. The data are under reduction.

Another new window for asteroseismology will be available with space experiments. COROT, the first experiment of stellar seismology from space (Baglin et al. 1998), will be launched by the end of 2002. It will allow to observe an extended set of stars ($4 \leq m_v \leq 9$) over long periods (up to 150 days) in order to make possible a detailed seismological investigation of the physical processes at work in stellar interiors.

Acknowledgements. C. Barban would like to thank M.J Goupil and B. Mosser for useful discussions. We thank G. Houdek and R. Samadi for amplitude predictions for Procyon A and discussions.

Appendix A: estimate of the visibility coefficients

In the case of observations of the velocity oscillations by measuring the Doppler shift of spectra lines, the oscillation velocity field is predominantly in the radial direction in the stellar atmosphere for the p modes and can be written by (e.g. Christensen-Dalsgaard 1996):

$$V(\theta,\phi;t) = \sqrt{4\Pi} Re\{V_0 Y_\ell^m(\theta,\phi) e^{-i(\omega_0 t - \delta_0 + m\Omega t)} \mathbf{a_r}\} \quad \text{(A1)}$$

where Re{z} is for the real part of a complex quantity z, V_0 is the intrinsic amplitude of the mode, $Y_\ell^m(\theta,\phi)$ are spherical

harmonics of degree l and azimuth m, (r, θ, ϕ) are spherical rotational coordinates: r is the distance to the stellar centre, θ the colatitude (i.e., the angle from the rotational axis) and ϕ the longitude, ω_0 is the initial pulsation, t is the time, δ_0 is the initial phase, Ω is the rotational velocity of the star and $\mathbf{a}_r$ is the unit vector in the radial direction.

In the case of whole-disk Doppler velocity observations, the velocity oscillation is obtained as the average of the velocity projected on the line of sight over the disk of the star:

$$V(t) = \frac{1}{A}\int_A V(\theta,\phi;t)cos(\theta)dA \tag{A2}$$

where A is the area on the disk.

In the coordinate system where the rotational axis points towards the observer, only the harmonic associated to m=0 has a non-zero contribution. Thus, the formula (A2) becomes for m=0:

$$V(t) = S_{\ell 0}^{(V)} V_0 \cos(\omega_0 t - \delta_0) \tag{A3}$$

where

$$S_{\ell 0}^{(V)} = 2\sqrt{2\ell+1}\int_0^{\Pi/2} P_\ell(\cos\theta)\cos^2\theta\sin\theta d\theta \tag{A4}$$

where $S_{\ell 0}^{(V)}$ is the velocity response function and P_ℓ is a Legendre function.

Following Gouttebroze & Toutain (1994), the response corresponding to a different choice of polar axis is obtained using transformation formulae connecting spherical harmonics corresponding to different orientations of the coordinate system:

$$S_{\ell m}^{(V_*)} = c_{mm'}^{\ell} S_{\ell m'}^{(V)} \tag{A5}$$

where $S_{\ell m}^{(V_*)}$ is the response corresponding to the coordinate system (θ_*, ϕ_*). As $S_{\ell m'}^{(V)}$=0 for m'$\neq$0, the Eq. (A5) becomes:

$$S_{\ell m}^{(V_*)} = c_{m0}^{\ell} S_{\ell 0}^{(V)} \tag{A6}$$

where

$$c_{m0}^{\ell} = (\frac{4\Pi}{2\ell+1})^{1/2} Y_\ell^m(\theta_*,\phi_*) \tag{A7}$$

Then, amplitude ratios between (l=0,m=0) and the other modes, i.e. $(S_{\ell m}^{(V_*)})/(S_{00}^{(V_*)})$, can be determined (see Table 3).

For this calculation, we assume that all the modes have the same intrinsic amplitude (V_0) and we neglect the transversal motions and the limb darkening.

References

Alexander D.R., Ferguson J.W., 1994, ApJ 437, 879

Audard N., Kupka F., Morel P., Provost J., Weiss W.W., 1998, A&A 335, 954

Baglin A., COROT team, 1998, International Astronomical Union. In: Deubner F.-L., Christensen-Dalsgaard J., Kurtz D. (eds.) Symposium no. 185, New Eyes to See Inside the Sun and Stars. Kyoto, Japan, 18–22 August, p. 301

Barban C., Martic M., Schmitt J., et al., 1999, In: Hearnshaw J.B., Scarfe C.D. (eds.) Proc. IAU colloquiun 170: Precise stellar radial velocities. Victoria BC Canada, ASP Conference Series in press

Bedford D.K., Chaplin W.J., Coates D.W., et al., 1995, MNRAS 273, 387

Bedford D.K., Chaplin W.J., Coates D.W., et al., 1993, In: Brown T.M. (ed.) GONG 1992: Seismic Investigation of the Sun and Stars. ASP Conf. Ser. Vol. 42, Brigham Young, Utah, p. 383

Böhm - Vitense E., 1958, Zeitschr. f. Astrophys. 46, 108

Breger M., Pamyatnykh A.A., Pikall H., Garrido R., 1999, A&A 341, 151

Brown T.M., 1999, In: Hearnshaw J.B., Scarfe C.D. (eds.) Proc. IAU colloquiun 170: Precise stellar radial velocities. Victoria BC Canada, ASP Conference Series in press

Brown T.M., Gilliand R.L., Notes R.W., Ramsey L.W., 1991, ApJ 368, 599

Caughlan G.R., Fowler W.A., 1988, Atomic Data and Nuclear Data Tables 40, 284

Chaboyer B., Demarque P., Guenther D.B., 1998, In: Bradley P.A., Guzik J.A. (eds.) A Half-Century of Stellar Pulsation Interpretations. ASP Conference Series Vol. 135, p. 67

Christensen-Dalsgaard J., 1996, Lecture Notes on Stellar oscillations

Christensen-Dalsgaard J., Berthomieu G., 1991, In: Solar interior and atmosphere. Tucson, AZ, University of Arizona Press, p. 401

Christensen-Dalsgaard J., 1982, MNRAS 199, 735

Eggleton P.P., Faulkner J., Flannery B.P., 1973, A&A 23, 325

Fekel F.C., 1997, PASP 109, 514

Fernandes J., Lebreton Y., Baglin A., 1996, A&A 311, 127

Fuhrmann K., Pfieffer M., Frank C., Reetz J., Gehren T., 1997, A&A 323, 909

Gelly B., Grec G., Fossat E., 1986, A&A 164, 383

Girard T.M., 1998, private communication

Girard T.M., Wu H., Lee J.T., et al., 1996, BAAS 188, 6002

Gouttebroze P., Toutain T., 1994, A&A 287, 535

Grevesse N., 1991, In: Michaud G., Tutukov A. (eds.) IAU Symp. 145, Evolution of Stars: The photospheric abundance connection. Kluwer, 63

Guenther D.B., Demarque P., 1993, ApJ 405, 298

Houdek G., 1998, private communication

Houdek G., Balmforth N.J., Christensen-Dalsgaard J., Gough D.O., 1999, A&A, accepted

Houdek G., Rogl J., Balmforth N., Christensen-Dasgaard J., 1995, In: Ulrich R.K., Rhodes Jr. E.J., Däppen W. (eds.) Proc. GONG'94: Helio- and astero- seismology from Earth and Space. PASC 76, San Francisco, p. 641

Iglesias C.A., Rogers F.J., Wilson B.G., 1992, ApJ 397, 717

Innis J.L., Isaak G.R., Speake C.C., Brazier R.I., Williams H.K., 1991, MNRAS 249, 643

Kjeldsen H., Bedding T.R., 1995, A&A 293, 87

Lebreton Y., Perrin M.N., Cayrel R., Baglin A., Fernandes J., 1999, A&A, submitted

Libbrecht K.G., 1988, IAUS 132, 83

Maeder A., 1983, A&A 120, 113

Martic M., Schmitt J., Lebrun J.-C., et al., 1999, A&A, accepted

Morel P., 1997, A&AS 124, 597

Mosser B., Maillard J.P., Mékarnia D., Gay J., 1998, A&A 340, 457

Perryman M.A.C., Brown A.G.A, Lebreton Y., et al., 1998, A&A 331, 81

Schaller G., Schaerer D., Meynet G., Maeder A., 1992, A&AS 96, 269

Smalley B., Dworetsky M.M., 1995, A&A 293, 446

Unno W., Osaki Y., Ando H., Shibahashi H., 1979, Nonradial Oscillations of Stars. University of Tokyo Press

van't Veer-Menneret C., Bentolila C., Katz D., 1998, In: Contrib. Astron. Obs. Skalnaté Pleso 27, 223